Cell, Vol. 86, 961–972, September 20, 1996, Copyright ©1996 by Cell Press

Autocatalytic Subunit Processing Couples Active Site Formation in the 20S Proteasome to Completion of Assembly

Ping Chen and Mark Hochstrasser
Department of Biochemistry and Molecular Biology
The University of Chicago
Chicago, Illinois 60637

Summary

The eukaryotic 20S proteasome is responsible for the degradation of many cellular proteins, but how it is assembled and how its distinct active sites are formed are not understood. Like other proteasome subunits, the yeast Doa3 protein is synthesized in precursor form. We show that the N-terminal propeptide is required for Doa3 incorporation into the proteasome and, remarkably, that the propeptide functions in *trans*, suggesting it serves a chaperone-like function in proteasome biogenesis. Propeptide processing is not required for proteasome assembly but is needed for maturation of a specific subset of active sites. The likely nucleophile for these sites is provided by the N-terminal threonine of mature Doa3. Additional data indicate that precursor processing is autocatalytic and requires association of the two halves of the proteasome particle, thereby preventing formation of proteolytic sites until the central hydrolytic chamber has been sealed off from the rest of the cell.

Introduction

The proteasome is the principal enzyme responsible for nonlysosomal protein degradation in most eukaryotic cells (Peters, 1994; Hochstrasser, 1995). Myriad cellular regulatory mechanisms depend on degradation of specific proteins, and the proteasome has been implicated in many of these proteolytic events. Misfolded or damaged proteins are also thought to be targeted to the proteasome. Finally, proteasomes are involved in the generation of peptides for the MHC class I antigen presentation pathway.

Four heptameric rings stack into a hollow cylinder to form the 20S proteasome (Peters, 1994). In the archaeon Thermoplasma acidophilum, a 20S proteasome with two related subunits, α and β, has been described; seven α subunits are in each of the outer two rings and seven β subunits in each inner one. A 2-fold (C2) symmetry axis relates one pair of α and β rings to the second pair. The more numerous eukaryotic 20S proteasome subunits are all related in sequence to the archaeal subunits, and based on electron microscopic reconstructions, the eukaryotic and prokaryotic particles are very similar in structure. In the yeast Saccharomyces cerevisiae, seven genes encode α-type subunits, and seven genes encode β-type subunits; yeast 20S proteasomes each contain 14 different subunits (Chen and Hochstrasser, 1995). A number of regulatory factors associate with 20S proteasomes, principal among them a 19S particle that confers ATP- and ubiquitin-dependence on proteolysis by the protease (Peters, 1994).

Recently, the Thermoplasma proteasome crystal structure was solved at 3.4 Å (Löwe et al., 1995). The active sites were localized to the β subunits on the inner surface of a central chamber in the particle. Importantly, the walls of the cylinder have no large openings, limiting entry of (unfolded) protein substrates to a set of narrow channels leading from the two ends of the particle. The Thermoplasma proteasome is a threonine protease, with the catalytic Thr residue located at the N-terminus of the β subunit (Löwe et al., 1995; Seemüller et al., 1995). When eukaryotic proteasomes are treated with lactacystin, an irreversible proteasome inhibitor, two sites in one of the β subunits are rapidly modified, one site being the N-terminal Thr residue (Fenteany et al., 1995). If it is assumed that the latter modification is what inactivates the enzyme, it would imply a comparable catalytic mechanism exists in eukaryotic and Thermoplasma proteasomes. Only three of the seven different eukaryotic β-type subunits in a given 20S particle appear to have all the necessary residues required for peptide bond hydrolysis (Seemüller et al., 1995).

The Thermoplasma protease also differs from the eukaryotic proteasome in that the archaeal enzyme has a single kind of active site, the eukaryotic particle at least three. The archaeal protease cleaves model peptides only after hydrophobic residues (a "chymotrypsin-like" activity); the eukaryotic protease can, in addition, cleave peptides after basic residues ("trypsin-like" activity) and after acidic residues ("peptidylglutamyl peptide hydrolyzing" [PGPH] activity). It is not known why the eukaryotic 20S proteasome has these distinct kinds of catalytic sites or how exactly they relate to the many different proteasome subunits. Adding further to the puzzle of subunit heterogeneity is the finding that in mammals, three variant β-type subunits, LMP2, LMP7, and MECL-1, are inducible by γ-interferon and can replace certain other proteasome subunits. LMP2 and LMP7 are important for presentation of certain class I antigens (reviewed in Hochstrasser, 1995).

We have begun to address aspects of 20S proteasome function in yeast. An earlier study led to a model for active site formation whose key feature was that interactions between specific subunits across the central β-subunit rings were critical for the establishment of individual active sites (Chen and Hochstrasser, 1995). This speculative model received significant support from the crystallographic data (see Hochstrasser et al., 1995). We also found that two β-type proteasome subunits, Doa3/Pre2/Prg1 and Pre3, are synthesized with N-terminal propeptides (Chen and Hochstrasser, 1995). Interestingly, the three kinds of eukaryotic β-type subunits thought to be "active" from the Thermoplasma studies are predicted to be processed by closely related mechanisms (Chen and Hochstrasser, 1995; Seemüller et al., 1995). Studies in mammalian cells suggest that proteasomes are assembled by an ordered pathway. A relatively long-lived ~15S assembly intermediate, which appears to be a half-proteasome, has been documented, and many of the subunits in this intermediate are in precursor form (Frentzel et al., 1994; Yang et al., 1995).

In the current work, we show that the Doa3 propeptide is critical for assembly of the yeast 20S proteasome in vivo. The propeptide of another β subunit cannot substitute for the Doa3 leader sequence. Most remarkably, the Doa3 propeptide functions in *trans*, allowing incorporation of the mature domain of Doa3 into the proteasome. This suggests that the β-subunit propeptide functions as a subunit-specific chaperone in proteasome biogenesis. We demonstrate that the N-terminal threonine of Doa3 is essential for the chymotrysin-like active sites of the proteasome. Pseudoreversion analysis indicates that Doa3 and Pre1, another subunit important for chymotrypsin-like activity, associate at the interface between the dyad-related halves of the proteasome, as predicted by the model mentioned above. Strikingly, a mutation in Pre1 that disrupts this interaction both inactivates the chymotrypsin-like active sites and inhibits proDoa3 processing. Failure to process proDoa3 does not prevent its incorporation into 20S particles but blocks activation of chymotrypsin-like activity. These results provide a structural solution to the problem of how premature activation of the proteasome is prevented during intermediate steps of assembly. Active site-bearing subunits remain in inactive precursor form until association of the two halves of the proteasome particle, which triggers the autocatalytic removal of the propeptides and final maturation of the proteasome active sites.

Results

The Propeptide of Doa3 Is Required for Incorporation of Doa3 into the Proteasome

We constructed a derivative of *DOA3*, *doa3ΔLS*, that has the sequence encoding the proDoa3 leader sequence (LS) deleted (Figure 1A). A plasmid with the *doa3ΔLS* allele was transformed into the *doa3Δ* [YCp50-DOA3] strain MHY784 (Table 1). The YCp50DOA3 plasmid carries both the wild-type *DOA3* gene and *URA3*, the latter conferring sensitivity to 5-fluoroorotic acid (FOA). The YCp50DOA3 plasmid cannot be lost from MHY784 cells because *DOA3* is essential for growth. If the *doa3ΔLS* allele on the second plasmid conferred Doa3 function, the YCp50DOA3 plasmid would become dispensible. This was not the case, however; the *doa3ΔLS* allele was unable to restore viability on FOA to MHY784 cells (Figure 1B, left).

The mutant *doa3ΔLS* allele was expressed in wild-type cells to determine whether sufficient amounts of Doa3 protein were being made and if so, whether the mutant protein was able to incorporate into 20S proteasomes. To distinguish the mutant protein from endogenous Doa3, we constructed a gene encoding a derivative of Doa3ΔLS with six histidines at its C-terminus; the tagged protein can be recognized specifically by an antiserum raised against His_6-tagged human LMP7, a proteasome subunit closely related to Doa3 (Chen and Hochstrasser, 1995). Wild-type Doa3 bearing this tag is fully functional. Expression of Doa3-His_6 derivatives was detected by immunoblot analysis; untagged Doa3 protein is at most only weakly recognized (Figures 1C and 1D, first lanes).

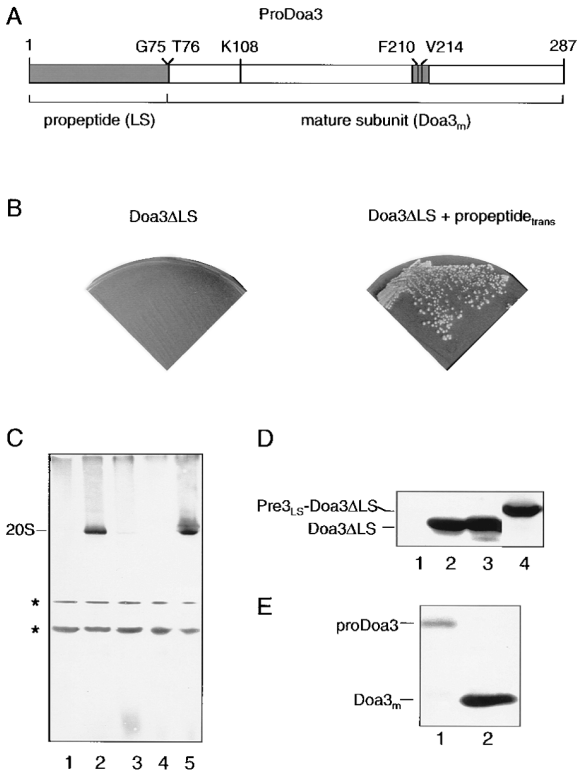

Figure 1. The Doa3 Propeptide Is Required for Doa3 Incorporation into the 20S Proteasome and Can Function In *Trans*

(A) Schematic of the Doa3 protein. For brevity, the N-terminal 75-residue propeptide is abbreviated as LS (for leader sequence) in some places in the text. Residues of Doa3 that were mutated in the current study are shown with their single-letter designations. Amino acid numbers refer in all cases to positions in proDoa3, even when the propeptide was synthesized separately from $Doa3_m$. Residues 208–218 of Doa3, which are predicted to correspond to helix 3 of the Thermoplasma 20S proteasome β subunit, are shaded dark gray.

(B) Growth on FOA of MHY784 cells (*doa3-Δ1::HIS3* [YCp50DOA3]) transformed with either YCpUbΔLSDOA3-His alone (left) or with YCpUbΔLSDOA3-His and $YEpDOA3_{LS}$ (right).

(C) Nondenaturing PAGE of extracts from congenic yeast cells expressing different alleles of *DOA3* followed by anti-LMP7-His_6 immunoblot analysis. Cells expressed the following Doa3 proteins from plasmid-borne alleles: lane 1, wild-type (untagged) Doa3 (MHY784); lane 2, Doa3-His_6 (MHY803); lane 3, Doa3ΔLS-His_6 (MHY784 carrying YCpUbDOA3ΔLS-His); lane 4, $Pre3_{LS}$-Doa3ΔLS-His_6 (MHY784 carrying YEpPRE3LS-DOA3ΔLS-His), and lane 5, Doa3ΔLS-His_6 plus Doa3LS (MHY952). The position of the 20S proteasome particle, based on anti-20S immunoblotting (data not shown), is indicated. Asterisks, two unidentified proteins that cross-react with the anti-LMP7-His_6 antiserum.

(D) SDS–PAGE and anti-LMP7-His_6 immunoblot analysis of the samples shown in panel C, lanes 1–4, showing the steady state levels of the different Doa3 derivatives.

(E) Pulse-labeling of cells expressing either Doa3-His_6 (MHY803, lane 1) or Doa3ΔLS-His_6 plus Doa3LS (MHY952, lane 2). Proteins were precipitated with anti-LMP7-His_6.

Whereas wild-type Doa3-His_6 was incorporated into the 20S particle, as assayed by nondenaturing polyacrylamide gel electrophoresis (PAGE) (Figure 1C, lane 2), the leaderless Doa3-His_6 protein was not (lane 3). Failure of Doa3ΔLS to incorporate into proteasomes was not due to poor protein expression. The amount of tagged Doa3ΔLS protein (Figure 1D, lane 3) was comparable to

Table 1. Yeast Strains

Strain	Genotype
MHY605[a]	*MATα his3-11 leu2-3,112 ura3Δ5 pre1-1 can^R*
MHY784	*MATα his3-Δ200 leu2-3,112 ura3-52 lys2-801 trp1-1 doa3-Δ1::HIS3* [YCp50DOA3]
MHY785	*MATa his3-Δ200 leu2-3,112 ura3-52 lys2-801 trp1-1 doa3-Δ1::HIS3* [YCp50DOA3]
MHY803	*MATα his3-Δ200 leu2-3,112 ura3-52 lys2-801 trp1-1 doa3-Δ1::HIS3* [YCplac22DOA3-His]
MHY907	*MATα his3 leu2-3,112 ura3 trp1-1 doa3-Δ1::HIS3 pre1-1* [YCp50DOA3]
MHY915	*MATα his3-Δ200 leu2-3,112 ura3-52 lys2-801 trp1-1 doa3-Δ1::HIS3* [YCplac22doa3-G75A-His]
MHY916	*MATα his3-Δ200 leu2-3,112 ura3-52 lys2-801 trp1-1 doa3-Δ1::HIS3* [YCplac22doa3-T76S-His]
MHY952	*MATα his3-Δ200 leu2-3,112 ura3-52 lys2-801 trp1-1 doa3-Δ1::HIS3* [YEpDOA3$_{LS}$][YCpUbDOA3ΔLS-His]
MHY969	*MATα his3 leu2-3,112 ura3 trp1-1 doa3-Δ1::HIS3 pre1-1* [YCplac22DOA3-His]
MHY970	*MATα his3-Δ200 leu2-3,112 ura3-52 lys2-801 trp1-1 doa3-Δ1::HIS3* [YCplac22doa3-F210A-His]
MHY971	*MATα his3 ura3 leu2-3,112 trp1-1 lys2-801 doa3-Δ1::HIS3 pre1-1* [YCplac22doa3-F210A-His]
MHY972	*MATα his3-Δ200 leu2-3,112 ura3-52 lys2-801 trp1-1 doa3-Δ::HIS* [YEp1DOA3$_{LS}$][YCpUbdoa3ΔLS-K108A-His]
MHY973	*MATα his3-Δ200 leu2-3,112 ura3-52 lys2-801 trp1-1 doa3-Δ1::HIS* [YEp1DOA3$_{LS}$][YCpUbdoa3ΔLS-T76A-His]
MHY975	*MATα his3 ura3 leu2-3,112 lys2-801 trp1-1 doa3-Δ1::HIS3 pre1-1* [YEp1DOA3$_{LS}$][YCpUbDOA3ΔLS-His]
MHY1003	*MATα his3-Δ200 leu2-3,112 ura3-52 lys2-801 trp1-1 doa3-Δ1::HIS3* [YCplac22doa3-T76A-His]
MHY1019	*MATα his3 leu2-3,112 ura3 trp1-1 lys2-801 pre1-1 doa3-Δ1::HIS3* [YCplac111doa3-V214A-His]
MHY1037	*MATα his3 leu2-3,112 ura3 trp1-1 lys2-801 pre1-1 doa3-Δ1::HIS3* [YEplac195doa3-F210A-His]
MHY1038	*MATα his3-Δ200 leu2-3,112 ura3-52 lys2-801 trp1-1 doa3-Δ1::HIS3* [YCplac111doa3-V214A-His]

[a] Same as strain 95-4-5D from D.H. Wolf.

that of tagged wild-type Doa3 in control cells (lane 2). Therefore, the Doa3 propeptide is necessary for assembly of Doa3 into the proteasome, a finding that contrasts with results with the simpler archaeon protease, which assembles properly even when the β subunit is synthesized without its propeptide (Zwickl et al., 1994).

The propeptides of different β-type subunits differ significantly in length and sequence. However, propeptides are not well conserved even between interchangeable mammalian β subunits despite close sequence similarity of the mature portions. Hence, it is unclear whether the variation among leader sequences reflects subunit-specific functions for these propeptides or is due to limited constraints on their structure (or both). To address this issue, we replaced the normal propeptide of Doa3 with the propeptide from Pre3. This fusion protein was expressed from either a low- or high-copy plasmid in the *doa3Δ* [YCp50DOA3] strain MHY784. Transformants were transferred to FOA plates to determine whether the Pre3$_{LS}$-Doa3ΔLS fusion could replace the normal Doa3 protein. No colonies were observed (data not shown). Expression of Pre3$_{LS}$-Doa3ΔLS in wild-type *DOA3* cells showed that the hybrid protein was being expressed at high levels (Figure 1D, lane 4). Interestingly, the protein migrated on SDS gels at a size consistent with the unprocessed fusion protein. Pre3$_{LS}$-Doa3ΔLS did not integrate into 20S particles (Figure 1C, lane 4). These results indicate that the function of proteasome β subunit propeptides is subunit-specific.

The Doa3 Propeptide Functions In *Trans*

From the above results, we could not exclude the possibility that Doa3ΔLS fails to function because of some unexpected consequence of its mode of synthesis. This concern would be eliminated if conditions were found in which the propeptide-less Doa3 were active. Specifically, Doa3ΔLS might function when the Doa3 propeptide is supplied as a separate peptide. There are a number of documented cases of propeptides from microbial proteases that can function when synthesized separately from the mature portion of the protease (see Discussion).

We designed a plasmid, YEpDOA3$_{LS}$, from which the sequence encoding the Doa3 propeptide could be separately expressed. YEpDOA3$_{LS}$ has no overlap in its *DOA3* DNA sequence with the Doa3ΔLS-encoding YCpUbDOA3ΔLS-His plasmid. YEpDOA3$_{LS}$ and YCpUbDOA3ΔLS-His were cotransformed into the MHY784 strain. The resulting transformants grew at wild-type rates on FOA plates (Figure 1B, right). This indicated that the YCp50DOA3 plasmid could be lost from the cells, in striking contrast to what was observed in the absence of YEpDOA3$_{LS}$ (Figure 1B, left). MHY952 cells (*doa3Δ* [YEpDOA3$_{LS}$] [YCpUbDOA3ΔLS-His]) grew indistinguishably from wild-type cells under several conditions (Table 2). Doa3ΔLS-His$_6$ was incorporated into 20S proteasomes in the presence of the *trans*-expressed propeptide (Figure 1C, lane 5) (the fate of the propeptide was not determined). To exclude the (unlikely) possibility that these results could be explained by illegitimate DNA recombination between the Doa3LS- and Doa3ΔLS-encoding plasmids, we pulse-labeled cells and immunoprecipitated the His$_6$-tagged Doa3 proteins. After a 15 min radiolabeling, most of the protein expressed from the wild-type *DOA3* gene was still in a precursor form (Figure 1E, lane 1); in contrast, only mature-sized Doa3 was detected in MHY952 cells (lane 2). We conclude that the Doa3 propeptide can function in *trans* in proteasome biogenesis.

Incorporation of Processing-Defective proDoa3 into the 20S Proteasome

The Doa3 propeptide is required for Doa3 function but is not present in the mature 20S proteasome. Previously, we derived a consensus sequence for proteasome β-subunit processing in which the only absolutely conserved residues were the Gly and Thr residues flanking the scissile bond (Chen and Hochstrasser, 1995). We therefore examined the consequences of altering these two residues for proteasome function in vivo (Figure 1A).

None of the three *doa3* alleles generated was lethal, but the mutant cells (MHY915, MHY916, and MHY1003) grew poorly, particularly the MHY1003 strain bearing

Table 2. Growth Rates of Mutant Strains Relative to Wild-Type Cells

Strain	Relevant Genotype	30°C	4°C	37°C	canav.
MHY784	*DOA3*	++++	+	++++	++++
MHY803	*DOA3-His*	++++	+	++++	++++
MHY915	*doa3-G75A-His*	+	−	−	−
MHY916	*doa3-T76S-His*	+	−	−	−
MHY1003	*doa3-T76A-His*	+/−	−	−	−
MHY907	*pre1-1 DOA3*	++	−	−	−
MHY969	*pre1-1 DOA3-His*	++	−	−	−
MHY970	*PRE1 doa3-F210A-His*	+++	+	+++	+++
MHY971	*pre1-1 doa3-F210A-His*	++	−	+	+
MHY1037	*pre1-1 doa3-F210A-His*[a]	++	ND	++	++
MHY1019	*pre1-1 doa3-V214A-His*	++++	+	+++	+++
MHY1038	*PRE1 doa3-V214A-His*	+++	+	+++	+++
MHY952	*DOA3ΔLS DOA3LS*	++++	+	++++	++++
MHY972	*doa3ΔLS-K108A-His DOA3LS*	++	−	−	−
MHY973	*doa3ΔLS-T76A-His DOA3LS*	++	−	−	−
MHY975	*pre1-1 DOA3ΔLS-His DOA3LS*	++	−	+	−

[a] Mutant *doa3-F210A* allele expressed from high copy plasmid. ND, not determined.

the *doa3-T76A* allele (Table 2). All the mutants also failed to grow at 37°C and were hypersensitive to canavanine and storage at 4°C (Table 2). The extremely poor growth of *doa3-T76A*-expressing cells made them difficult to work with, so we concentrated our analysis on the other two *doa3* mutants. Pulse–chase experiments revealed severe defects in propeptide removal from the doa3-G75A and doa3-T76S proteins in MHY915 and MHY916 cells, respectively (Figure 2A). While wild-type proDoa3 is processed with a half-time of ~20 min, little if any processing of either mutant protein was detected after a 40 min chase. At steady state, the majority of wild-type Doa3 was in the mature form (Figure 2B, lane 2). In contrast, both the doa3-G75A and doa3-T76S proteins were present largely as unprocessed polypeptides (lanes 3 and 4), although a trace amount of protein apparently comigrating with $Doa3_m$ (mature form) was detectable.

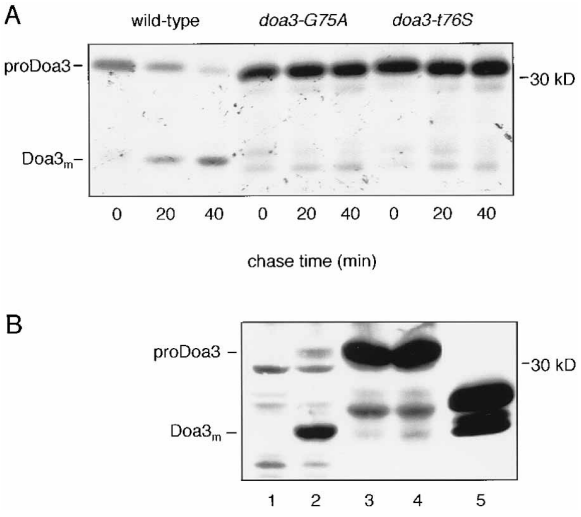

Figure 2. Substitutions of the Residues Flanking the Scissile Bond in the proDoa3 Processing Site Inhibit Propeptide Cleavage

(A) Pulse-chase analysis comparing the rate of wild-type proDoa3 processing to that of the doa3-G75A and doa3-T76S mutant proteins. All proteins bear the C-terminal His_6 tag and were precipitated with anti-LMP7-His_6 antibodies. Cells were pulse-labeled for 15 min. (B) Anti-LMP7-His_6 immunoblot analysis of Doa3 mutants. The cells expressed the following Doa3 proteins from plasmid-borne alleles: lane 1, wild-type (untagged) Doa3; lane 2, Doa3-His_6; lane 3, doa3-His_6-G75A; lane 4, doa3-His_6-T76S; and lane 5, purified 20S proteasomes from doa3-His_6-G75A-expressing cells. Positions of the Doa3 primary translation product (proDoa3) and mature Doa3 ($Doa3_m$) are indicated.

To study the consequences of proDoa3 processing defects for proteasome assembly and enzymatic activity, we analyzed proteasomes that had been fractionated on glycerol gradients. We focused on the *doa3-G75A* mutant (MHY915) because the mutation is not in the mature portion of Doa3, so any observed defects would be more readily attributable to the perturbation in proDoa3 processing. Gradient fractions of wild-type cell extracts were run on nondenaturing gels followed by immunoblotting. When blots were probed with either an anti-20S proteasome antibody (Figure 3A, left) or an antibody that specifically recognizes Doa3-His_6 (data not shown), proteasomes were found in the rapidly sedimenting protein fractions, peaking in fraction 5. Parallel samples fractionated by SDS–PAGE and analyzed by immunoblotting showed that all the detectable Doa3-His_6 protein in the 20S particles was in the processed form (Figure 3B, left). The peaks of PGPH and chymotrypsin-like activities coincided with the peak of 20S particles in fraction 5 (Figure 3C, left).

PGPH activity levels in the 20S proteasome peak fractions from *doa3-G75A* cell extracts (Figure 3C, right) were comparable to or slightly higher than the level observed in wild-type cells. In contrast, chymotrypsin-like activity in the fractions from *doa3-G75A* cells was reduced ~10-fold relative to wild-type. The (undiminished) PGPH activity peak was at the same position in the wild-type and *doa3-G75A* fractionations, arguing that fully assembled 20S proteasomes exist in wild-type and mutant cells. Nondenaturing PAGE partially dissociated the mutant proteasomes into subcomplexes, however (Figure 3A). Significantly fewer full-size 20S particles were seen on such gels when using extracts from *doa3-G75A* cells instead of wild-type cells, and several new fast-migrating species were observed in the mutant

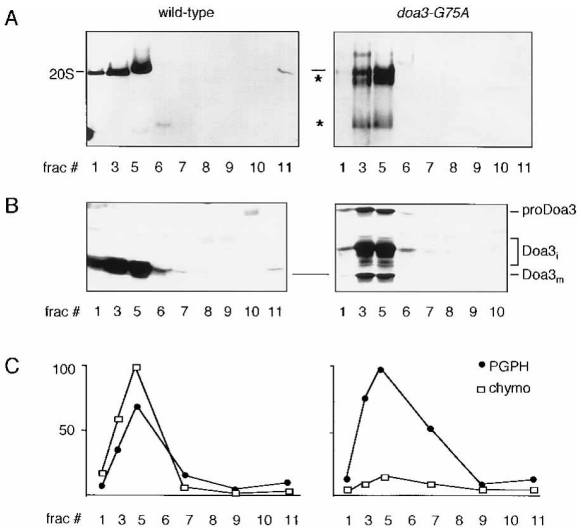

Figure 3. Failure to Process proDoa3 Does Not Prevent Its Incorporation into 20S Particles but Prevents Formation of the Chymotrypsin-like Active Sites

(A) Anti-20S proteasome immunoblot analysis of nondenaturing gels loaded with proteins from wild-type (MHY803) and *doa3-G75A* (MHY915) cell extracts that had been separated on 10%-40% glycerol gradients. Asterisks mark proteasomal subparticles that are only detected in the mutant proteasome fractions; the slow-migrating species in lane 3 may be an aggregate of proteasomes or proteasome subparticles.

(B) Anti-LMP7-His_6 immunoblot analysis of proteins separated by SDS-PAGE from the same fractions used in (A). Positions of the Doa3 primary translation product (proDoa3), mature Doa3 ($Doa3_m$), and intermediate-sized processed forms of Doa3 ($Doa3_i$) are indicated. The excess of proDoa3 seen if mutant cells are immediately lysed in SDS sample buffer is not evident in the fractionations. Much of the protein could be present as large aggregates, which may be difficult to collect from the gradient tubes.

(C) The defect in proDoa3 processing causes loss of chymotrypsin-like (chymo) but not PGPH activity (average of duplicate measurements). Values were normalized to maximal activity in wild-type and mutant cells, respectively.

20S fractions (asterisks in Figure 3A; the film for the right panel was overexposed to make the novel species more readily visible). Thus, it appears that the proDoa3 processing defect caused by the *doa3-G75A* mutation does not block 20S proteasome assembly, but the resulting particle is structurally less stable than its wild-type counterpart.

A significant amount of unprocessed proDoa3 was observed in the *doa3-G75A* proteasome fractions (Figure 3B, right), confirming that a failure to process proDoa3 does not prevent its incorporation into 20S proteasomes. Much of the protein detected by the anti-LMP7-His_6 antibody, however, migrated as a cluster of bands ($Doa3_i$) whose mobility was intermediate between that of proDoa3 and the small fraction of Doa3 that migrated near the position of mature Doa3. The $Doa3_i$ species are most likely generated by cleavage in the Doa3 propeptide since the antibody will not recognize Doa3 without the C-terminal His_6-tag. The major $Doa3_i$ band coincided with a minor band observed when cells were directly lysed in SDS sample buffer (Figure 2B, lanes 3 and 4). The extended sample preparation under nondenaturing conditions required for gradient fractionation resulted in a higher ratio of (mis)processed to unprocessed species than did immediate cell lysis under denaturing conditions. This suggests that the $Doa3_i$ species were generated primarily during in vitro sample preparation.

This last inference is supported by an analysis of 20S proteasomes purified from *doa3-G75A* cells by a multistep purification protocol (Chen and Hochstrasser, 1995). This extensive procedure yielded 20S particles in which virtually no unprocessed proDoa3 was detectable (Figure 2B, lane 5). The yield of mutant 20S particles was more than 10-fold lower than that of wild-type particles purified in parallel, indicating that the mutant proteasomes were sensitive to one or more steps in the procedure. This suggests that the particles were structurally unstable, as had been inferred from the glycerol gradient analysis (Figure 3A). When purified doa3-G75A proteasomes were examined on silver-stained 2-D gels, the pattern of spots was comparable to that of wild-type proteasomes, but the mature Doa3 species was reduced at least 10-fold relative to the other subunits (data not shown). The purified doa3-G75A proteasomes had no chymotrypsin-like activity, while PGPH activity appeared to be unimpaired (data not shown).

We conclude from these results that removal of the Doa3 propeptide is critical for activation of the chymotrypsin-like active sites of the proteasome but is not essential for assembly of the 20S particle or formation of other kinds of active sites. However, the failure to correctly process proDoa3 results in a structurally abnormal particle, which leads to its instability in vitro and, possibly, to the severe growth defects of the mutant strains.

Role of Specific Doa3 Residues in the Chymotrypsin-like Activity of the Proteasome

Experiments with the Thermoplasma proteasome strongly suggested that the side chain of the N-terminal threonine of the β subunit serves as the active site nucleophile in peptide bond cleavage; the α-amino group was also implicated in the catalytic mechanism (Löwe et al., 1995; Seemüller et al., 1995). By analogy to the archaeon enzyme, the N-terminal threonine of $Doa3_m$ (Thr-76) may be a key residue for the chymotrypsin-like sites in the yeast 20S proteasome.

Although the data presented above demonstrate that correct processing of proDoa3 is important for the chymotrypsin-like activity of the yeast proteasome, they do not directly address the question of whether the N-terminal Thr of $Doa3_m$ is a critical residue for this activity. The difficulty in establishing a role for Thr-76 in the catalytic function of the mature proteasome results from the fact that the Doa3 propeptide is essential for proteasome assembly (Figure 1) and that Thr-76 is also part of the processing site "substrate" (Figure 2). To circumvent these problems, we took advantage of the ability of the Doa3 propeptide to function in *trans*, eliminating the need for precursor processing altogether. To this end, a yeast strain, MHY973, was created in which sequences encoding the Doa3 propeptide and the

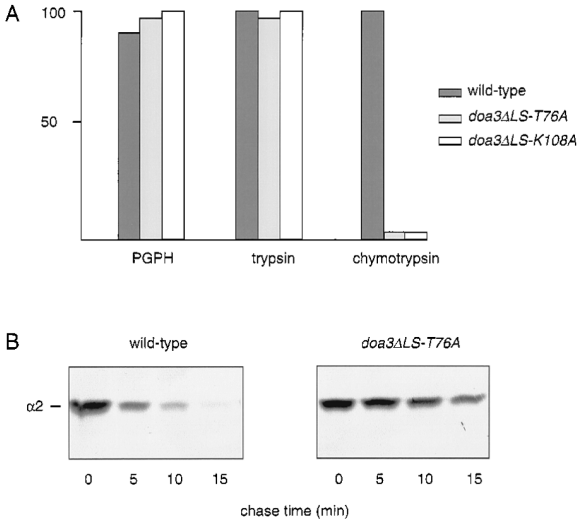

Figure 4. The N-terminal Thr Residue of Doa3 Is Essential for a Specific Active Site of the Proteasome

(A) Comparison of three major peptidase activities in proteasomes isolated by glycerol gradient fractionation of extracts from *doa3ΔLS doa3LS* (wild-type, MHY952), *doa3ΔLS-T76A doa3LS* (MHY973), and *doa3ΔLS-K108A doa3LS* (MHY972) cells (average of duplicate measurements).

(B) Pulse–chase analysis of α2 degradation in MHY952 (wild-type) and MHY973 (*doa3ΔLS-T76A doa3LS*) cells.

doa3ΔLS-T76A polypeptide were separately expressed by a strategy analogous to that described earlier.

MHY973 cells had only a mild growth defect, unlike MHY1003 cells, which expressed the full-length mutant doa3-T76A protein and were barely viable (Table 2). 20S proteasomes isolated from MHY973 cell extracts by glycerol gradient fractionation were indistinguishable from wild-type 20S particles on nondenaturing gels (data not shown). However, the mutant proteasomes had no detectable chymotrypsin-like activity, whereas the PGPH and trypsin-like activities were unimpaired (Figure 4A). Thus, a failure to properly process proDoa3 has much more profound effects on cell growth and proteasome function than does inactivation of the chymotrypsin-like active sites per se. We also measured the degradation in MHY973 cells of a known in vivo substrate of the 20S proteasome, the MATα2 repressor (Chen and Hochstrasser, 1995). The MATα2 protein was stabilized ~6-fold in the mutant (Figure 4B).

Further support for the similarity in catalytic mechanisms of the yeast and Thermoplasma proteasomes was provided by additional mutagenesis experiments. Mutation of Lys-33 in the archaeal β subunit eliminated peptide-cleaving activity without detectably altering the structure of the proteasome (Seemüller et al., 1995). The cocrystal structure of the archaeon proteasome complexed with a peptide inhibitor suggests that Lys-33 functions either as the proton acceptor during nucleophilic attack or to orient/polarize other chemical groups for catalysis (Löwe et al., 1995). A Lys residue corresponding to Lys-33 of the archaeon β subunit is found in all the eukaryotic β-type subunits predicted to have an active site N-terminal threonine in their mature forms. We therefore created strains that expressed doa3 derivatives in which the relevant lysine, Lys-108, was changed to alanine either in the context of full-length Doa3 or in Doa3ΔLS; in the latter case, the propeptide was again supplied in *trans*. MHY972 cells, which expressed doa3ΔLS-K108A and Doa3LS, had a moderate growth defect (Table 2). 20S proteasomes from these cells were obtained by glycerol gradient fractionation. As in strain MHY973, the mutant proteasomes were stable during nondenaturing PAGE, had undiminished PGPH and trypsin-like activities, but were devoid of chymotrypsin-like activity (Figure 4A). Therefore, Lys-108 of Doa3, like Thr-76, is essential for the chymotrypsin-like activity of the mature 20S proteasome. Mutation of Lys-108 to Ala in full-length Doa3 (*doa3-K108A*) was lethal (data not shown). The inviability of *doa3-K108A* cells was in contrast to the modest growth defect of the *doa3ΔLS-K108A doa3LS* strain. These two strains differ only in the former's requirement for propeptide processing, suggesting that Lys-108 is essential for the processing of proDoa3.

In summary, two key residues implicated in the catalytic mechanism of the archaeal proteasome appear to have analogous functions in the Doa3 subunit for the chymotrypsin-like active sites of the yeast proteasome.

Doa3 and Pre1 Interact at the Interface between the Two Central Proteasome Rings

The chymotrypsin-like activity of the yeast proteasome can be virtually eliminated by mutations in two different β subunits, Doa3/Pre2 and Pre1 (Heinemeyer et al., 1991). This suggests that the yeast proteasome contains a single kind of chymotrypsin-like active site to which both Doa3 and Pre1 contribute. Our earlier analysis of mutant *doa3* proteasomes had led us to propose a model for the active sites in the eukaryotic proteasome in which specific subunit contacts between the two inner β-type subunit rings contribute to the formation of particular active sites (Chen and Hochstrasser, 1995) (see Figure 7). For instance, we postulated that Doa3 and Pre1 interacted at the interface between the two β-subunit rings in a way that was crucial for configuration of the chymotrypsin-like active sites. The Doa3 subunit appears to have most or all of the residues involved directly in catalysis (see above), so Pre1 in this model would contribute primarily to substrate binding and/or stabilization of the active site pocket.

Subsequently, we noted that the Ser-to-Phe substitution resulting from the yeast *pre1-1* mutation is at a position in Pre1 that maps, assuming structural homology to the Thermoplasma proteasome, to a helix at the surface between the β-subunit rings in the prokaryotic enzyme (helix H3). Residues in the H3 helices of one β-subunit ring interact across a dyad axis with the H3 helices in the other β-subunit ring. The bulky Phe substitution in the pre1-1 subunit might interfere sterically with proper packing of the H3 helix against the dyad-related H3 helix from a subunit in the other β-subunit ring. If our model were correct, this other subunit would be Doa3, and it might therefore be possible to suppress defects associated with *pre1-1* by making compensatory mutations in the H3 helix of Doa3.

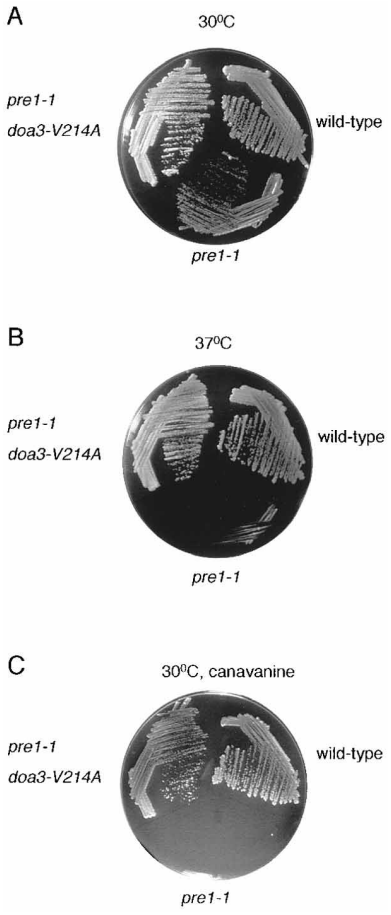

Figure 5. Pseudoreversion Analysis Demonstrates Apposition of the Doa3 and Pre1 Subunits at the Interface between the Inner Rings of the Proteasome

(A) Growth at 30°C on SD plates. The strains for (A)–(C) are as follows: wild-type, MHY803; *pre1-1*, MHY969; and *pre1-1 doa3-V214A*, MHY1019.

(B) Growth at 37°C on SD plates.

(C) Growth at 30°C on SD plates containing 0.6 μg/ml canavanine sulfate.

Based on sequence alignment, the putative H3 helix of Doa3 spans residues 208–218 (Figure 1A). Assuming three-dimensional structural similarity as well, the side chains of Phe-210 and Val-214 are expected to project toward the β-ring interface (see Figure 1 in Löwe et al., 1995). We therefore generated mutant *doa3* alleles that encoded proteins with Ala substitutions at these positions and tested them for their ability to suppress the mutant *pre1-1* phenotype, which includes slow growth at 30°C, temperature-sensitivity, and hypersensitivity to canavanine (Heinemeyer et al., 1991). Strikingly, both *doa3* mutations suppressed the *pre1-1* abnormalities, albeit to different degrees (Table 2; Figure 5). Better suppression was observed with *doa3-V214A*, and the degree of suppression was the same when the *doa3-V214A* allele was on either a low- or high-copy plasmid (Figure 5 and data not shown). Double mutants between *doa3-F210A* and *pre1-1* showed partial reversion of the *pre1-1* phenotype, and the suppression was enhanced when the *doa3-F210A* allele was expressed from a high-copy plasmid. In the absence of *pre1-1*, both *doa3-V214A* and *doa3-F210A* caused only mild defects (Table 2 and data not shown).

Suppression of the *pre1-1* mutation was allele-specific. The *doa3-1* mutation (Chen and Hochstrasser, 1995), which does not perturb helix H3, resulted in inviability when combined with *pre1-1*. We also generated a mutant *pre3* allele encoding a protein in which the Phe residue corresponding to Phe-210 of Doa3 was replaced by an Ala residue. Unlike overexpression of *doa3-F210A* (or, to a lesser degree, *doa3-F210G*; data not shown), high-copy expression of *pre3-F152A* failed to suppress the *pre1-1* phenotype (data not shown).

In summary, our results not only demonstrate a close similarity between archaeal and eukaryotic proteasome structures at the molecular level but also suggest that contacts between the Doa3 and Pre1 subunits at the interface between the dyad-related β-subunit rings are crucial for the chymotrypsin-like activity of the yeast proteasome.

Disruption of the Pre1-Doa3 Dyad Contact Inhibits proDoa3 Processing

Based on the finding that ~15S precursor particles contained unprocessed β subunits while mature proteasomes did not, Frentzel et al. (1994) concluded that subunit processing occurs in the precursor particles. However, it remains possible that processing occurs at a step after the 15S particle stage. Circumstantial evidence suggests proteasome β-subunit processing might be autocatalytic, but direct data for this are lacking. As shown above, formation of the chymotrypsin-like active sites in the yeast proteasome requires interaction of Doa3 and Pre1 subunits between the central two subunit rings. If proDoa3 subunit processing were autocatalytic, i.e., dependent on formation of an active site–like structure in proDoa3, such processing should also require proper association of proDoa3 and Pre1 between the symmetry-related halves of the proteasome. A strong prediction of this hypothesis is that normal processing of proDoa3 should be impaired in *pre1-1* cells because of the defect in Pre1-Doa3 interaction. This was precisely what was observed (Figures 6A and 6B). Pulse-chase analyses revealed a level of inhibition in proDoa3 processing approaching that observed when the propeptide cleavage site had been directly mutated (compare Figure 6A to Figure 2A). Interestingly, at steady state, a species apparently comigrating with $Doa3_m$ was present in comparable amounts in wild-type and *pre1-1* cells, although the bulk of Doa3 in *pre1-1* cells was in the precursor form (Figure 6B).

If the defect in proDoa3 processing in *pre1-1* cells were a result of the inability of the pre1-1 and Doa3 subunits to interact normally across the proteasome dyad axis, restoration of that interaction by second-site mutations in Doa3 (Figure 5) should at least partially rescue proDoa3 processing. Consistent with this, processing was largely restored in *pre1-1* cells when the Doa3 precursor carried the V214A substitution (Figure 6A). These data strongly suggest that proDoa3 processing requires proper interaction between proDoa3

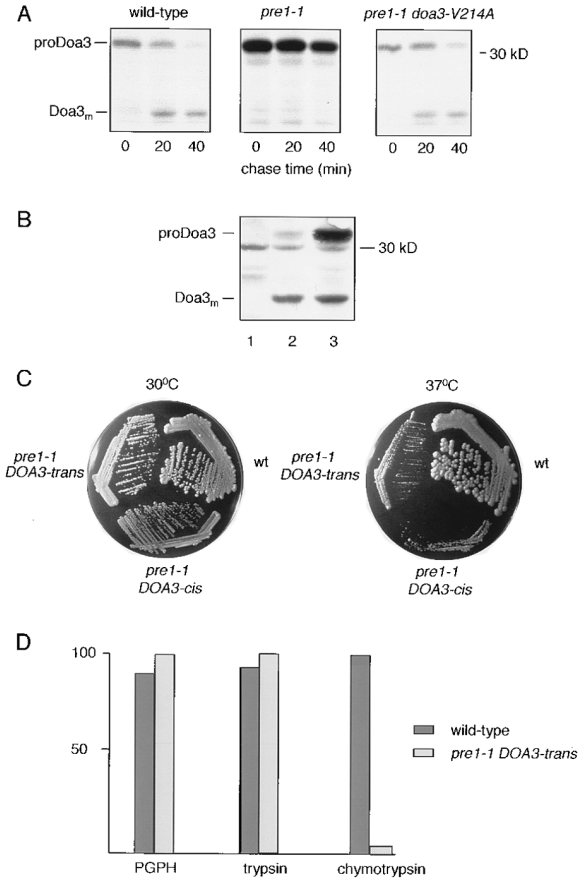

Figure 6. Proper Interaction between the Inner Rings of the Proteasome Is Required for proDoa3 Subunit Processing and for Function of the Mature Proteasome

(A) Pulse–chase analysis of proDoa3-His_6 processing in wild-type (MHY803), *pre1-1* (MHY969), and *pre1-1 doa3-V214A* (MHY1019) cells. Cells were pulse-labeled for 15 min. Proteins were precipitated with anti-LMP7-His_6 antibodies.

(B) Anti-LMP7-His_6 immunoblot analysis of proDoa3 processing in *pre1-1* cells. Extracts were made from (1) *PRE1* cells expressing wild-type (untagged) Doa3 (MHY784), (2) *PRE1* cells expressing Doa3-His_6 (MHY803), and (3) *pre1-1* cells expressing Doa3-His_6 (MHY969).

(C) Growth at 30°C and 37°C on YPD plates of wild-type (wt, MHY803), *pre1-1 DOA3* (*Doa3-cis*, MHY969) and *pre1-1 doa3ΔLS doa3LS* cells (*Doa3-trans*, MHY975), the latter expressing the Doa3 propeptide from a separate plasmid.

(D) Peptidase activities of proteasomes isolated by glycerol gradient fractionation of extracts from wild-type (MHY803) and *pre1-1 doa3ΔLS doa3LS* cells (MHY975).

and Pre1 across the β-subunit rings, in assembled 20S particles.

It is conceivable that the primary defect in *pre1-1* cells is the failure to process properly the Doa3 precursor, thereby causing the defect in chymotrypsin-like activity of 20S proteasomes (Figure 3). This leaves open the possibility that proDoa3 and Pre1 normally associate directly only transiently during proteasome assembly, at which time the propeptide is removed. To resolve this ambiguity, we tested the effect of the *pre1-1* mutation on proteasomes that do not require proDoa3 processing because the cells (MHY975) express Doa3LS and Doa3ΔLS. MHY975 cells remained hypersensitive to canavanine and were sensitive to high temperature, although growth at both 30°C and 37°C was somewhat better than when Doa3 was synthesized in its normal precursor form (strain MHY969) (Figure 6C; Table 2). These data indicate that the *pre1-1* mutation causes a defect in 20S proteasomes containing mature Doa3. This inference was confirmed biochemically by assaying peptidase activities of proteasomes isolated by gradient fractionation (Figure 6D). The chymotrypsin-like activity of MHY975 20S proteasomes was <5% that of the wild-type particles, while the trypsin-like and PGPH activities were unimpaired.

We conclude from these data that the Doa3 and Pre1 subunits interact at the interface between the two central β-subunit rings in the mature 20S proteasome and that this interaction is crucial for formation of the chymotrypsin-like active sites. Because precisely the same interaction with Pre1 is required for proDoa3 processing, these results further suggest that an active site–like structure in proDoa3 is required for propeptide cleavage, i.e., that β-subunit precursor processing is autocatalytic.

Discussion

In this study, we provide evidence that distinct active sites of the eukaryotic 20S proteasome are formed by specific interactions between different proteasome subunits and that these sites are only activated when the two halves of the 20S particle have associated correctly. Such association triggers the autocatalytic removal of β-subunit propeptides, thereby revealing the new N-termini responsible for substrate cleavage. Proteasome biogenesis requires the β-subunit propeptide, which, surprisingly, can function in *trans*.

Subunit Arrangement in the Eukaryotic Proteasome

Immunoelectron microscopy was used to localize several eukaryotic α and β subunits to the outer and inner rings, respectively, of the 20S proteasome (Kopp et al., 1993, 1995); these data supported earlier inferences about the similarity of eukaryotic proteasome architecture to that of the Thermoplasma enzyme. However, none of the relative positions of any of the 28 subunits in the eukaryotic proteasome was known from previous work. Taking advantage of the published data on the Thermoplasma proteasome crystal structure (Löwe et al., 1995), we devised a structure-based, site-specific pseudoreversion strategy to identify an interaction between the Doa3 and Pre1 subunits across the central rings of the proteasome (Figures 5 and 6). Because of the dyad symmetry of the proteasome, two such Doa3-Pre1 pairings must exist (see Figure 7).

The suppression data provide striking support for the idea that the general structural similarity between the eukaryotic 20S proteasome and the much simpler archaeal version of the same enzyme extends to the molecular level, at least for the subunit–subunit interactions investigated here. From a complementary perspective, the present results can be seen to provide strong genetic

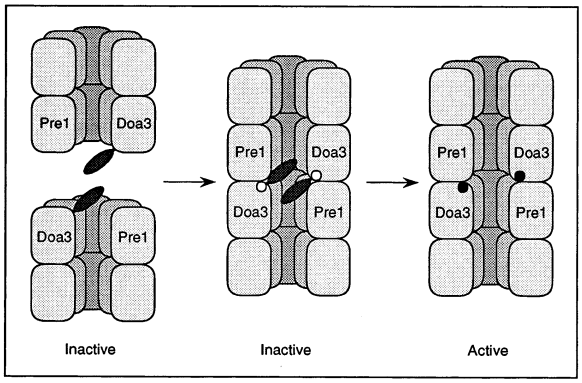

Figure 7. Model for Autocatalytic Proteasome β-Subunit Processing and the Coupling of Active Site Formation to Full Proteasome Assembly

A cutaway view of the proteasome is shown, and the Doa3-Pre1 interaction is highlighted (the relative positions of the two Doa3-Pre1 subunit pairs within the central rings are not known). The intermediate shown has an as-yet-uncharacterized active site structure (denoted as open circles) capable of autocatalytic subunit processing but not efficient substrate cleavage. Only following propeptide removal is the mature active site structure (closed circles) obtained. See text for details.

evidence for the correctness of the Thermoplasma proteasome structure model. The pseudoreversion strategy described here can be generalized to determine the precise spatial arrangement of all subunits in the eukaryotic 20S proteasome. Knowledge of proteasome quaternary structure will be critical for the formulation and evaluation of models of how the many different eukaryotic proteasome subunits contribute to protein breakdown. It will also be needed to understand how β-subunit replacements in proteasomes alter proteasome function; examples of such replacements include those occurring in the mammalian MHC class I antigen presentation pathway or during early Drosophila development (Peters, 1994).

Active Sites of the Eukaryotic Proteasome

The Doa3–Pre1 interaction between the middle rings of the proteasome is required specifically for chymotrypsin-like activity. An obvious question is how such subunit interactions actually contribute to substrate binding and/or hydrolysis. In the Thermoplasma proteasome, the catalytic residues are not in direct contact with dyad-related β subunits (Löwe et al., 1995). Unless there are major structural rearrangements during the catalytic cycle, this interface, particularly that formed between H3 helices, cannot be directly involved in catalysis. It is more likely that formation in Doa3 of a stable substrate-binding pocket or the proper positioning of residues important for peptide cleavage is dependent on its interaction with the dyad-related Pre1 subunit.

A number of Thermoplasma β-subunit residues known to be essential for proteolysis are not conserved in Pre1; however, given their overall sequence similarity, Pre1 is still likely to form a cleft or pocket that might bind substrate. Substrate binding by such "inactive" subunits may contribute to several characteristic properties of the proteasome, such as its processivity and its tendency to generate peptides with a narrow length distribution (see Hochstrasser, 1995). If substrate dissociation from noncatalytic binding sites, e.g. in Pre1, were slow, particularly when the site is attached to a free end of a polypeptide, the bound substrate could be cleaved at active sites in neighboring subunits. This would tend to generate peptides with a limited range of sizes. Whether subunits with catalytically inactive binding pockets are somehow coupled to particular active subunits within the proteasome is unknown.

Cells bearing proteasomes devoid of detectable chymotrypsin-like activity show a significant decrease (~6-fold) in the rate of degradation of MATα2, a known substrate of the ubiquitin-proteasome pathway (Figure 4). Much more dramatic stabilization of α2 (as much as 15-fold) has been seen in certain other proteasome mutants and in yeast strains lacking particular ubiquitin-conjugating enzymes (Chen et al., 1993; DeMarini et al., 1995). Therefore, the chymotrypsin-like sites are important but not absolutely essential for degradation of α2 by the ubiquitin-proteasome pathway. This suggests that multiple distinct active sites contribute to protein degradation, not just a single subset of sites defined by cleavage of model peptides.

The *DOA3* mutagenesis data (Figure 4) provide strong evidence that the eukaryotic proteasome, like the Thermoplasma enzyme, is a threonine protease. The N-terminal threonine and a specific lysine (Lys-108) in Doa3, which correspond to residues directly implicated in the archaeal catalytic mechanism, are essential for the chymotrypsin-like active sites of the mature yeast proteasome. Previously, the rate of modification by lactacystin of subunit X/MB1, the mammalian homolog of yeast Doa3, was shown to correlate closely with inactivation of the chymotrypsin-like activity in purified proteasomes (Fenteany et al., 1995). The N-terminal threonine of X/MB1 was modified by the compound, but because a second X/MB1 residue was also modified, it was not possible to conclude that it was the N-terminal modification that caused the inhibition. The data in Figure 4 indicate that the threonine is indeed the critical residue. It is important to note that this conclusion could not have been drawn if we had restricted the analysis to the full-length proDoa3 protein because this threonine is also part of the target site for precursor cleavage.

Coupling of Active Site Formation to Full Assembly of the 20S Proteasome

As described in the Introduction, the central proteolytic chamber of the 20S proteasome is sealed off from the cell except through very narrow openings at the ends of the cylinder. Prior to full assembly of the particle, however, indiscriminate proteolysis of cellular proteins must be prevented by other means. Two potential solutions are readily imagined. One posits that active sites are kept inactive by the N-terminal propeptides, which are only removed late in the assembly pathway. The other supposes that stable active sites can only form in the fully assembled complex. Our data indicate that both mechanisms operate and, moreover, that they are tightly coupled (Figure 7).

The inference that only the completely assembled particle has proteolytic activity is based on the finding that even in proteasomes that do not require proDoa3 processing, perturbation of the interface between the dyad-related Doa3 and Pre1 subunits causes a severe defect in chymotrypsin-like activity and in the ability of cells to withstand a variety of stresses (Figure 6 and Table 1). Hence, proper contacts between the two halves of the proteasome must be maintained even after assembly and subunit processing have been completed. This could serve as a fail-safe mechanism to prevent unregulated protein destruction were the particle to dissociate partially. There is no evidence that the *pre1-1* mutation affects any component of the proteasome other than the chymotrypsin-like active sites (Figure 6) (Heinemeyer et al., 1991).

Doa3 and several other β subunits are synthesized in precursor form, and failure to remove the Doa3 propeptide specifically blocks activation of the chymotrypsin-like sites (Figure 3). Preliminary data indicate that mutation of the proPre3 processing site specifically inhibits PGPH activity (P. C. and M. H., unpublished data). Thus, these propeptides may behave as active site–specific inhibitors. Although this would seem to be unnecessary given that full particle assembly is usually required for active site formation, a weak peptide hydrolytic activity has been reported in irregular protein aggregates formed by purified Thermoplasma β subunits that lacked propeptides (Zwickl et al., 1994). There may be conditions in vivo under which eukaryotic β-type subunits without leader sequences could also associate improperly to form partially active complexes. The propeptides may help prevent such aberrant complexes from forming or may block proteolytic activity should they form.

Association of proteasome half-dimers leads to the autocatalytic removal of the inhibitory β-subunit propeptides, resulting in proteasome activation. Although final proof of autocatalytic processing will require a demonstration of processing by purified proteasome components, the genetic and biochemical data presented here provide strong evidence that this is the case, as argued in the Results. Based on the Thermoplasma proteasome-inhibitor cocrystal structure, Löwe et al. (1995) suggested that the free α-amino group serves as the proton acceptor during nucleophilic attack on the substrate. If this is true, propeptide cleavage must require a slightly rearranged active site structure since the α-amino group is not available in the precursor. A structural framework that could explain the autoprocessing of several proteins, including proteasome β subunits, has recently been proposed (Brannigan et al., 1995). The ϵ-amino group of the residue corresponding to Lys-108 in Doa3 is also favorably positioned to serve as the proton acceptor; it may function as such during processing. We showed that mutation of Lys-108 to Ala in $Doa3_m$ (coexpressed with the *trans*-complementing propeptide) eliminates chymotrypsin-like activity in the mature proteasome; the same mutation in proDoa3 is lethal, consistent with a role in processing.

Interestingly, whenever processing of proDoa3 was perturbed, the cellular levels of proDoa3 in mutant cells greatly exceeded the total amount of wild-type Doa3 in congenic strains (Figures 2A and 2B and 6B). This suggests the existence of a feedback mechanism that results in increased expression when proteasome function or processing is inhibited. The mechanistic basis of this phenomenon remains to be explored, but one attractive possibility is that a positive regulator of *DOA3* expression is itself a substrate of the proteasome-dependent proteolytic pathway.

Function of Proteasome Subunit Propeptides

As just discussed, β-subunit propeptides act to inhibit the activity of specific catalytic sites in the proteasome. It is unlikely, however, that this is the essential function of the propeptide since proteasomes are normally only activated when the two proteasome halves have come together properly, at which time the propeptide is removed. Why, then, is the Doa3 propeptide required for cell survival? Results of the current work indicate that the propeptide functions as a chaperone. Chaperones are factors that facilitate the proper folding or assembly of other proteins but are not themselves part of the final protein structure. The Doa3 propeptide (Doa3LS) is required for incorporation of Doa3 into the proteasome particle (Figure 1). Because the *DOA3* gene is essential for viability, the inability to incorporate Doa3 into the proteasome is expected to be lethal, as was observed. Doa3LS cannot be replaced by the propeptide of another β-type subunit, Pre3, but it functions when synthesized separately from the mature domain of Doa3. These data imply that the propeptide can interact noncovalently with $Doa3_m$.

It is not yet known at what step(s) in proteasome biogenesis the Doa3 leader sequence is required. Potential steps include folding of the Doa3 subunit, targeting of Doa3 to its correct position in an early proteasome precursor particle, and/or alignment of the two β-subunit rings. It is noteworthy that, unlike the yeast Doa3 β-type subunit, the 8-residue propeptide of the Thermoplasma β subunit is dispensible for assembly of active proteasomes, at least in E. coli (Zwickl et al., 1994). The more complicated subunit composition of the eukaryotic proteasome makes it tempting to speculate that the leader sequences of eukaryotic β-type subunits have evolved to facilitate correct placement of subunits in the particle.

The synthesis of proteins with sequence elements that are eventually removed but are needed for the proteins to reach their mature, functional forms is extremely common. It is far more exceptional for such protein segments to be able to function in *trans* (Baker et al., 1993). Examples have been reported for a number of simple microbial proteases that are synthesized with large propeptides. Two of the best characterized are the secreted bacterial proteases subtilisin and α-lytic protease (Baker et al., 1993). In these cases, the N-terminal propeptide appears to function by catalyzing a late step in protein folding. The eukaryotic proteasome is the most complex particle known whose normal assembly has been shown to involve an intramolecular chaperone that can also function intermolecularly. The ability to manipulate the assembly pathway of the yeast proteasome genetically, as reported here, should provide a powerful way to study this novel class of chaperones and their role in cellular protein morphogenesis.

Experimental Procedures

Yeast and Bacterial Media and Methods

Yeast rich (YPD) and minimal plates (SD) plates were prepared as described, and standard methods were used for genetic manipulation of yeast (Chen et al, 1993). For all phenotypic tests, cells were initially grown for several days on rich medium at 30°C. Cells were tested for growth at 30°C on SD containing 0.6 μg/ml canavanine but lacking arginine and on either YPD or SD medium at 37°C. Survival of cells during storage at 4°C was evaluated by inoculating colonies into minimal medium from 1-week-old cultures kept at 4°C on YPD plates. E. coli strains used were MC1061 and JM101, and standard methods were employed for recombinant DNA work (Ausubel et al., 1989).

Construction of *doa3* Mutant Strains

Mutant alleles of *doa3* were generated by a two-step polymerase chain reaction (PCR) procedure starting with plasmid templates encoding either wild-type Doa3 or Doa3 with a C-terminal hexahistidine tag (Chen and Hochstrasser, 1995). Mutant alleles constructed in this way were cloned into YCplac22, except for the *doa3-V214A* allele, which was subcloned into YCplac111 and YEplac181 (Gietz and Sugino, 1988). Mutations were verified by DNA sequencing. To make the corresponding *doa3* strains, MHY784 cells were transformed with plasmids bearing the *doa3* alleles, and the transformants were plated on FOA to identify cells that had lost YCp50DOA3.

YCpUbDoa3ΔLS-His was constructed as follows. A ubiquitin gene, along with a *CUP1* promoter controlling its transcription, was PCR-amplified from YEp96 (Hochstrasser et al., 1991) with primers that introduced a BamHI site upstream of *CUP1* and a KpnI site that overlapped the last codon. A segment of *DOA3* downstream of the propeptide-encoding region of the open reading frame (ORF) was amplified from YCpUbDoa3ΔLS-His using a 5′ primer that introduced a silent mutation at codon 76 to create a KpnI site and a 3′ primer hybridizing downstream of a natural BamHI site after *DOA3*. Both PCR products were cut with KpnI and BamHI and were ligated to BamHI-cut YCplac22, creating an in-frame fusion of ubiquitin and $Doa3_m$ coding elements. The propeptide-encoding region of *DOA3* together with its upstream sequence was amplified and cloned into YEplac181 to create $YEpDOA3_{LS}$. The 3′ primer used for PCR provided an in-frame stop codon immediately after codon 75 of the *DOA3* ORF. YEpPRE3LSDOA3ΔLS was constructed by amplification of a DNA fragment bearing both *PRE3* upstream sequences and the region of the *PRE3* ORF encoding the Pre3 propeptide. This DNA fragment was ligated to the DNA fragment encoding mature Doa3 (described above) in YCplac22, and the HindIII–BamHI insert was subcloned into YEplac181.

To generate congenic *pre1-1* and *pre1-1 doa3* strains, MHY605 was crossed to MHY785, and *pre1-1 doa3-Δ1::HIS3 can*^{S} [YCp50-DOA3] segregants were identified. One such segregant, MHY907, was transformed with *TRP1*- or *LEU2*-based plasmids carrying the different *doa3* alleles, and the resulting transformants were plated on FOA to identify colonies that had lost YCp50DOA3. The *pre1-1 doa3-1* double mutant failed to form colonies on FOA at 23°C or 30°C.

Pulse–Chase and Immunoblot Analyses

Pulse–chase analysis was carried out as described (Chen et al., 1993). Immuno-precipitations were done with either an affinity-purified anti-α2 antibody, or an antiserum against a human $LMP7\text{-}His_6$ protein (Chen and Hochstrasser, 1995); the latter was a gift from Y. Yang. SDS–PAGE of proteins was carried out according to standard procedures (Ausubel et al., 1989). Nondenaturing 4%–15% gradient gels were prepared with a gradient maker using the same solutions used for SDS–PAGE except that SDS was omitted. 2-D PAGE was performed as described (Chen and Hochstrasser, 1995). For Western immunoblot analyses, cell extracts were prepared from exponentially growing yeast; procedures for immunoblotting were described previously (Chen and Hochstrasser, 1995). The anti-yeast 20S proteasome antiserum was a gift from K. Tanaka and was diluted 1:1500 in TBST (10 mM Tris–HCl [pH 8.0], 150 mM NaCl, 0.1% Tween-20). The anti-$LMP7\text{-}His_6$ antibody was diluted 1:1000 in TBST. Proteins were detected using ECL reagents from Amersham.

Protein Fractionation on Glycerol Gradients

For gradient fractionation of yeast extracts made under nondenaturing conditions, cells were grown to mid-log phase in 200 ml minimal medium. Based on OD_{600} measurements, equal numbers of cells were harvested and washed once in spheroplasting buffer (1 M sorbitol, 30 mM DTT, 50 mM Tris–HCl, [pH 8.0]). Cells were then incubated with 0.5 mg/ml zymolyase 100T (Seikagaku) in the same buffer for 30 min at 30°C. The spheroplasts were resuspended in 20S proteasome buffer (20 mM Tris–HCl [pH 8.0], 150 mM NaCl, 1 mM EDTA, 10% glycerol) and lysed by sonication. After removal of cell debris, extracts were loaded onto 10%-40% glycerol gradients made in 20S proteasome buffer, and the samples were centrifuged for 16 hr at 40,000 rpm in a Beckman SW41Ti rotor at 4°C. Fractions (1 ml) were collected, and aliquots were tested for peptide hydrolysis activities and by Western immunoblotting. Purification of yeast 20S proteasomes and peptide hydrolysis assays were carried out as described (Chen and Hochstrasser, 1995).

Acknowledgments

We would like to thank Y. Yang and K. Tanaka for antibodies; D. H. Wolf for the *pre1-1* yeast strain; and P. Johnson, L. Stillman, S. Swaminathan, and A. Turkewitz for many helpful comments on the manuscript. This work was supported by the National Institutes of Health (GM46904). P. C. was funded in part by NIH predoctoral training grant GM07183.

References

Ausubel, F.M., Brent, R., Kingston, R.E., Moore, D.D., Seidman, J.G., Smith, J.A., and Struhl, K. (1989). Current Protocols in Molecular Biology (New York: John Wiley and Sons).

Baker, D., Shiau, A.K., and Agard, D.A. (1993). The role of pro regions in protein folding. Curr. Opin. Cell Biol. *5*, 966–970.

Brannigan, J.A., Dodson, G., Duggleby, H.J., Moody, P.C.E., Smith, J.L., Tomchick, D.R., and Murzin, A.G. (1995). A protein catalytic framework with an N-terminal nucleophile is capable of self-activation. Nature *378*, 416–418.

Chen, P., and Hochstrasser, M. (1995). Biogenesis, structure, and function of the yeast 20S proteasome. EMBO J. *14*, 2620–2630.

Chen, P., Johnson, P., Sommer, T., Jentsch, S., and Hochstrasser, M. (1993). Multiple ubiquitin-conjugating enzymes participate in the in vivo degradation of the yeast MATα2 repressor. Cell *74*, 357–369.

DeMarini, D.J., Papa, F.R., Swaminathan, S., Ursic, D., Rasmussen, T.P., Culbertson, M.R., and Hochstrasser, M. (1995). The yeast *SEN3* gene encodes a regulatory subunit of the 26S proteasome complex required for ubiquitin-dependent protein degradation in vivo. Mol. Cell. Biol. *15*, 6311–6321.

Fenteany, G., Standaert, R.F., Lane, W.S., Choi, S., Corey, E.J., and Schreiber, S.L. (1995). Inhibition of proteasome activities and subunit-specific amino-terminal threonine modification by lactacystin. Science *268*, 726–731.

Frentzel, S., Pesold-Hurt, B., Seelig, A., and Kloetzel, P.-M. (1994). 20S proteasomes are assembled via distinct precursor complexes: processing of LMP2 and LMP7 proproteins takes place in 13–16S preproteasome complexes. J. Mol. Biol. *236*, 975–981.

Gietz, R.D., and Sugino, A. (1988). New yeast-Escherichia coli shuttle vectors constructed with in vitro mutagenized yeast genes lacking six-base pair restriction sites. Gene *74*, 527–534.

Heinemeyer, W., Kleinschmidt, J.A., Saidowsky, J., Escher, C., and Wolf, D.H. (1991). Proteinase yscE, the yeast proteasome/multicatalytic-multifunctional proteinase: mutants unravel its function in stress induced proteolysis and uncover its necessity for cell survival. EMBO J. *10*, 555–562.

Hochstrasser, M. (1995). Ubiquitin, proteasomes, and the regulation of intracellular protein degradation. Curr. Opin. Cell Biol. *7*, 215–223.

Hochstrasser, M., Ellison, M.J., Chau, V., and Varshavsky, A. (1991). The short-lived MATα2 transcriptional regulator is ubiquitinated in vivo. Proc. Natl. Acad. Sci. USA *88*, 4606–4610.

Hochstrasser, M., Papa, F.R., Chen, P., Swaminathan, S., Johnson,

P., Stillman, L., Amerik, A., and Li, S.-J. (1995). The DOA pathway: studies on the functions and mechanisms of ubiquitin-dependent protein degradation in the yeast *Saccharomyces cerevisiae*. Cold Spring Harbor Symp. Quant. Biol. *60*, 503–513.

Kopp, F., Dahlmann, B., and Hendil, K.B. (1993). Evidence indicating that the human proteasome is a complex dimer. J. Mol. Biol. *229*, 14–19.

Kopp, F., Kristensen, P., Hendil, K.B., Johnsen, A., Sobek, A., and Dahlmann, B. (1995). The human proteasome subunit HsN3 is located in the inner rings of the complex dimer. J. Mol. Biol. *248*, 264–272.

Löwe, J., Stock, D., Jap, B., Zwickl, P., Baumeister, W., and Huber, R. (1995). Crystal structure of the 20S proteasome from the archaeon T. acidophilum at 3.4 Å resolution. Science *268*, 533–539.

Peters, J.M. (1994). Proteasomes: protein degradation machines of the cell. Trends Biochem. Sci. *19*, 377–382.

Seemüller, E., Lupas, A., Stock, D., Löwe, J., Huber, R., and Baumeister, W. (1995). Proteasome from Thermoplasma acidophilum: a threonine protease. Science *268*, 579–582.

Yang, Y., Früh, K., Ahn, K., and Peterson, P.A. (1995). In vivo assembly of the proteasomal complexes, implications for antigen presentation. J. Biol. Chem. *270*, 27687–27694.

Zwickl, P., Kleinz, J., and Baumeister, W. (1994). Critical elements in proteasome assembly. Nature Struct. Biol. *1*, 765–769.